Journal of Applied Geophysics 132 (2016) 125–136

Contents lists available at ScienceDirect

Journal of Applied Geophysics

journal homepage: www.elsevier.com/locate/jappgeo

# Hydrothermal alteration and its effects on the magnetic properties of Los Pelambres, a large multistage porphyry copper deposit

Joseline Tapia [a,b,c,*], Brian Townley [c,d], Loreto Córdova [e], Fernando Poblete [c], César Arriagada [c]

[a] Mines Engineering Department, Engineering Faculty, University of Antofagasta, Chile
[b] Instituto de Ciencias de la Tierra, Facultad de Ciencias, Universidad Austral de Chile, Chile
[c] Geology Department, Faculty of Mathematical and Physical Sciences, University of Chile, Santiago, Chile
[d] Advanced Mining Technology Center, FCFM, Universidad de Chile, Chile
[e] OVDAS, Observatorio Volcanológico de los Andes del Sur, Rudecindo Ortega 03850, Temuco, Región de la Araucanía, Chile

ARTICLE INFO

*Article history:*
Received 2 October 2015
Received in revised form 15 April 2016
Accepted 6 July 2016
Available online 8 July 2016

*Keywords:*
Magnetic properties
Magnetic minerals
Hydrothermal alteration
Porphyry copper deposits
Los Pelambres deposit

ABSTRACT

The Los Pelambres porphyry copper deposit is located 190 km north of Santiago, Chile. A paleomagnetic and mineralogical study was conducted at this deposit to determine the effects of hydrothermal alteration on the magnetic properties and minerals of rocks within the deposit when compared to the surrounding country rock. In the Los Pelambres deposit, magnetic properties of rocks are carried by titano-hematite and titano-magnetite solid solution minerals, where the former commonly indicates the exsolution of rutile. Magnetic minerals of intrusive rocks from the greater Los Pelambres region show that magmatic titano-magnetites and magnetites are the main magnetization carriers. The hydrothermal fluid associated with rutile exsolution textures could have played an important role in the mineralization of Cu in this deposit. The paleomagnetic properties in the Los Pelambres deposit can be divided in three main groups: (i) HMRG (high magnetic remanence group), (ii) HMSG (high magnetic susceptibility group), and (iii) LMSG (low magnetic susceptibility/remanence group). *In-situ* magnetic properties of the HMSG and LMSG are similar to the formations and units present regionally, however HRMG samples clearly differ from the country rocks. The high variability of *in-situ* magnetic properties presented in the Los Pelambres deposit has also been characteristic of other porphyry copper deposits in Chile (e.g., Chuquicamata and El Teniente). Regarding the field of exploration geophysics and porphyry copper deposits, this study suggests that phyllic, chloritic, and potassic alterations are related to low, intermediate, and high *in-situ* NRM, respectively, suggesting that geophysical methods must target a noisy magnetic signal depending on the scale of the study. The knowledge and results obtained are especially meaningful because magnetic surveys conducted for exploration do not commonly allow for the detection of ore mineralization.


## 1. Introduction

Hydrothermal alteration processes indicate that mineral transformations are mostly controlled by fluid-rock interactions and are buffered by the pH and redox equilibrium (Reed, 1997). Mineral stability in hydrothermal ore deposits such as porphyry copper systems have a direct effect on the alteration of mineral associations, including ferromagnetic minerals (Astudillo et al., 2008; Riveros et al., 2014; Townley et al., 2007). Alteration mineral associations in porphyry copper systems are spatially and chronologically zoned (Lowell and Guilbert, 1970; Richards, 2003; Sillitoe, 2010); therefore the paleomagnetic properties of these alteration minerals may present spatial or temporal variations that are dissimilar from the country and host rock which can even differ between hydrothermal alteration zones or events (Alva-Valdivia et al., 2003a; Astudillo et al., 2010).

In porphyry copper systems, deposits of indisputable hydrothermal origin, Fe-Ti oxides, and sulfides are most commonly present (Beane and Titley, 1981; Brimhall, 1980; Meyer and Hemley, 1997; Richards, 2003; Sillitoe, 2010). Some of these minerals are capable of registering natural remanent magnetism (Astudillo et al., 2008, 2010, among others), an inherent property of ferromagnetic minerals. In general, porphyry copper deposits are hosted by older porphyritic intrusions or pre-existing rocks. These host rocks are characterized by an original ferromagnetic mineralogy from which initial, specific paleomagnetic properties derive that often change due to hydrothermal processes.

Most paleomagnetic studies of igneous rocks have been conducted on non-altered rocks, nevertheless some have explored the effects of hydrothermal alteration processes on the paleomagnetic properties of rocks (Alva-Valdivia and López-Loera, 2011; Alva-Valdivia et al., 2003a, 2003b; Astudillo et al., 2008, 2010; Faundez, 2002; Tapia, 2005;

* Corresponding author.
*E-mail address:* joseline.tapia@uach.cl (J. Tapia).

http://dx.doi.org/10.1016/j.jappgeo.2016.07.005
0926-9851/

Tassara et al., 2000; Taylor, 2000; Townley et al., 2007). Despite a poor understanding of the effects of hydrothermal alteration processes on the magnetic properties of porphyry copper systems, airborne and ground magnetic surveys can be used as tools for locating prospective deposits because of the magnetic properties of rocks and expected magnetic contrasts assumed from geophysical interpretation models. For instance, most aeromagnetic interpretations assume that natural remanent magnetism (NRM) represents an intensity of at least one order of magnitude less than the induced magnetic component, excluding NRM. Yet, paleomagnetic studies of northern Chile rocks have demonstrated that NRM represents at least 50% or more of the measured magnetic intensity (Arriagada et al., 2000, 2003; Somoza et al., 1999); hence, NRM vectors may represent an important component of the total measured magnetic field and disregarding these properties may cause a major bias when interpreting aeromagnetic data.

In this study of the Los Pelambres porphyry copper system, one of the largest multi-stage porphyry copper deposits of the central Chilean Andes Miocene copper belt (see Atkinson et al., 1996; Perelló et al., 2012; Sillitoe, 1973; Fig. 1a), results of paleomagnetic data and possible interpretations for this deposit are presented, expanding on similar studies in Chilean mines of stratabound deposits (Carolina de Michilla; Townley et al., 2007), iron oxides copper gold deposits (El Laco; Alva-Valdivia et al., 2003a and El Romeral; Alva-Valdivia et al., 2003b), and porphyry copper deposits (Chuquicamata; Astudillo et al., 2008, El Teniente; Astudillo et al., 2010, and La Escondida; Riveros et al., 2014). In particular, this survey presents the results of a general paleomagnetic and mineralogic study of the Los Pelambres porphyry copper deposit in order to evaluate (i) the effects of distinct hydrothermal and mineralization stages on the magnetic properties of rocks, (ii) the potential zonation of magnetic properties, and (iii) the overall expected magnetic contrast as a result of hydrothermal processes.

## 2. Regional and local geology

### 2.1. Regional geology

The Los Pelambres porphyry copper deposit is located 190 km north of Santiago within the main Andes Range (31°43′S; 70°70′W), between 2200 to 4500 m. a.s.l. The geology of the central zone of Chile, at the latitude of Los Pelambres, consists of stratified volcanic and sedimentary rocks whose ages span from the Middle Triassic until Recent, and intrusive bodies that range from the Cretaceous to the Miocene (Fig. 1b). Middle Triassic rocks correspond to greywackes and shales that are located along the western margin of the region (El Quereo Formation; Cecioni and Westermann, 1968; not shown on Fig. 1b). These are overlain by Jurassic volcanic rocks (Ajial and Horqueta Formations; Vergara et al., 1995), and continuing to the east by Cretaceous rocks: (ii) the Quebrada Marquesa Formation (Aguirre and Egert, 1961), a volcano-sedimentary sequence which occurs in the Precordillera, followed by (ii) both members of the Viñitas Formation (Rivano and Sepúlveda, 1991), constituted by lavas, tuffs, and breccias of andesitic composition with rhyolitic intercalations and calcareous sedimentary beds, and by

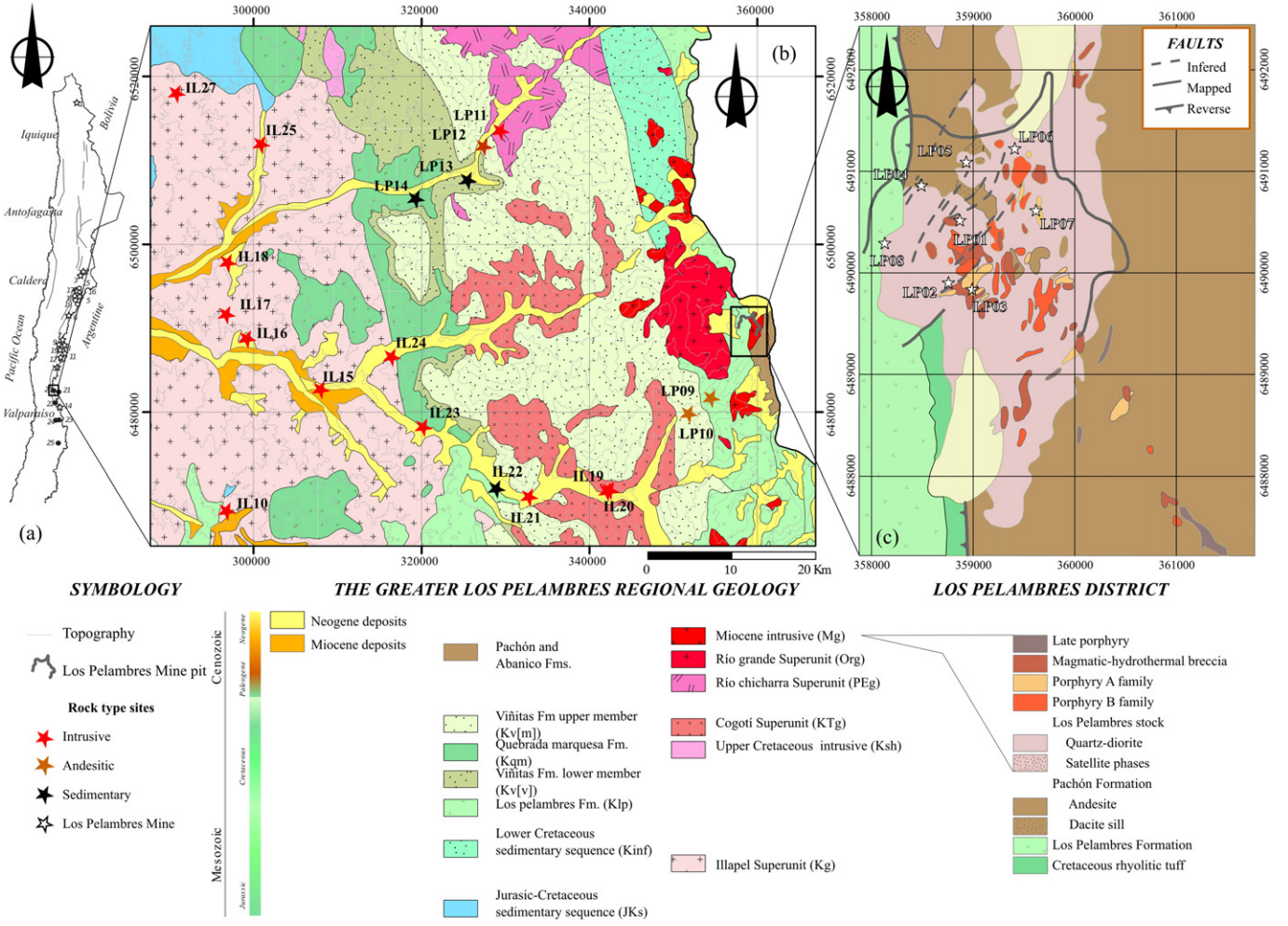


**Fig. 1.** Study area location and sampling sites. (a) Location of deposits within the Upper Miocene-lower Pliocene metallogenic belt of Chile; (b) The greater Los Pelambres region geology and sampling sites; (c) The Los Pelambres porphyry copper deposit local geology and sampling sites.

(iii) mafic to intermediate composition lavas of the Los Pelambres Formation (Rivano and Sepúlveda, 1991; Fig. 1b).

Cretaceous and Upper Cretaceous-Tertiary intrusive rocks include the Illapel Superunit (85.9–134 Ma; Rivano et al., 1985 and references therein) and Cogotí Superunit (35.4–67.1 Ma; Rivano et al., 1985 and references therein), which intrude the Lower Jurassic and Cretaceous basement respectively (Fig. 1b). Farther to the east, Miocene to Pleistocene volcanic rocks of the Farellones Formation (Aguirre, 1960; Rivano et al., 1990) and El Pachón Formation (Perelló et al., 2012) extend into Argentina, attributable to the interpreted eastward migration of the volcanic arc to its current position (Jordan et al., 1983). These rocks are intruded by Miocene stocks that show bimodal magmatism, as indicative of the Río Grande and Río Chicharra Superunits (8–26 Ma; Rivano et al., 1985 and references therein; Fig. 1b).

### *2.2. Los Pelambres porphyry copper deposit: geology, structures, and mineralization*

The precursor intrusion in this deposit was a north trending, 4.5 by 2.5 km$^2$, quartz-diorite stock known as Los Pelambres, where the mineralized multiphase porphyry bodies were emplaced (Perelló et al., 2012; Fig. 1c). The bulk of the stock is made up of light to medium gray, subequigranular to hypidiomorphic equigranular quartz-diorite, with a dominance of andesine over biotitized hornblende and biotite (Atkinson et al., 1996; Perelló et al., 2012). Many intermineral porphyry phases are also present in this deposit (Atkinson et al., 1996). Perelló et al. (2012) grouped these phases into A and B porphyries for practicality (Fig. 1c), which are comprised of dikes and small bodies of irregular geometry, the majority of which are clustered in the central part of the Los Pelambres stock (Perelló et al., 2012; Fig. 1c). Porphyry A intrusions are characterized by a dark brown, fine-grained andesitic composition, whereas Porphyry B dikes are distinguished by medium grain sized, porphyritic textures of dacitic composition (Perelló et al., 2012). Regarding magmatic and hydrothermal features, these are related to aplites, pegmatites, unidirectional solidification textures, magmatic-hydrothermal and igneous breccias, and copper, gold, and molybdenum mineralization (Perelló et al., 2012 and references therein).

The geologic structure dominating the Los Pelambres deposit is the Los Pelambres reverse fault: a N-striking, high angle, and brittle structure. In addition, a series of NE-striking, 55° to 70° SE-dipping faults, spatially associated with alteration and mineralization, cut the west-central part of the Los Pelambres stock (Perelló et al., 2012; Fig. 1c).

In relation to hydrothermal alteration and mineralization types, this deposit resembles those characteristic of other porphyry copper deposits (Camus, 2003; Gustafson and Hunt, 1975; Lowell and Guilbert, 1970; Richards, 2003; Sillitoe, 1997, 2010), in which a potassic core grades laterally to a sericitic zone surrounded by a propylitic halo (Atkinson et al., 1996; Perelló et al., 2012; Sillitoe, 1973). The potassic alteration is associated with the presence of hydrothermal biotite and potassium (K) feldspar with anhydrite, chalcopyrite, and to a lesser extent bornite, digenite, and molybdenite (Sillitoe, 1973). Hydrothermal magnetite is present locally at Los Pelambres (Perelló et al., 2012). Magmatic-hydrothermal and igneous breccias are part of the potassic alteration halo, in which brown and green biotites, sericite and to a lower degree chlorite, are present in their apical parts (Perelló et al., 2012). The sericitic alteration is superimposed on the potassic alteration, and is associated with quartz, sericite, pyrite, and tourmaline (schorl type; Sillitoe, 1973).

Six main veinlet types are recognized within the potassic zone, which from oldest to youngest are: (i) early biotite; (ii) green mica; (iii) type 4; (iv) type A; (v) type B; and (vi) type D veinlets (Atkinson et al., 1996; Perelló et al., 2012; Skewes and Atkinson, 1985).

This deposit also underwent supergene alteration and mineralization processes. Sulfide oxidation occurred at maximum depths of 350 m (Atkinson et al., 1996).

The multiple intrusion events of the Los Pelambres porphyry copper deposit have been studied by various authors (Atkinson et al., 1996; Bertens et al., 2003, 2006; Perelló et al., 2012; Sillitoe, 1973). Perelló et al. (2012) obtained ages of emplacement for the precursor quartz-diorite intrusion of 13.60 ± 0.30 and 13.00 ± 0.70 Ma (U-Pb in zircon), which is comparable to ages obtained previously by other authors (13.92 to 12.51 Ma U-Pb in zircon, Bertens et al., 2006; crystallization age range between 16 and 12 Ma U-Pb in zircon, Bertens et al., 2003). For the type A porphyry, emplacement ages range between 12.30 ± 0.30 and 10.80 ± 0.23 Ma (U-Pb in zircon; Perelló et al., 2012), and for the B porphyry, intrusion ages range between 11.50 ± 0.30 and 10.53 ± 0.14 Ma (U-Pb in zircon; Perelló et al., 2012). Atkinson et al. (1996) and Sillitoe (1973) dated alteration biotite by K-Ar, obtaining an alteration age of 9.9 ± 1 Ma and 9.85 Ma, respectively. Bertens et al. (2006) dated samples of igneous and hydrothermal muscovite, biotite, and hornblende by Ar-Ar, yielding an age of 10.58 to 9.52 Ma. The youngest event recorded in this deposit corresponds to supergene leaching and sulfide enrichment. Ar-Ar dating in jarosite determined an age of 5.34 Ma (Bertens et al., 2006), implying that the deposit was already unroofed at that time. Most jarosites were dated in the range ca. 3.06 to ca. 0.93 Ma, suggesting that the most intense supergene process occurred within that time interval (Bertens et al., 2006).

## 3. Paleomagnetic sampling and methodology

### *3.1. Sampling*

A total of 19 paleomagnetic sampling sites selected within unaltered regional lithological units surrounding the Los Pelambres district were sampled with a hand-held paleomagnetic mini core sampler (sites IL and LP09 to LP14; Fig. 1b, Table 1), and 80 paleomagnetic samples were collected in total. These samples were taken from sedimentary, volcanic, and intrusive rocks. Mini-core samples were oriented in the field, both magnetically and using the solar azimuth. At the Los Pelambres mine, a total of 20 oriented block samples were taken from 8 representative sites of the deposit (sites LP01 to LP08; Fig. 1c, Table 1) spanning all lithological and accessible alteration units. These blocks were reoriented at the Department of Geology, University of Chile, and drilled for a total of 27 paleomagnetic mini-cores, all oriented magnetically with respect to the original block orientation obtaining a total of 42 standard paleomagnetic rock specimens.

### *3.2. Alteration and ferromagnetic mineralogy: analytical techniques*

The alteration and ferromagnetic mineralogy of the Los Pelambres samples and ferromagnetic mineralogy of two representative sites of intrusive units (the Illapel and Cogotí Superunits) were studied using standard petrographic techniques and by analysis of the chemical composition and textures of silicates and Fe-Ti oxides using a SEM-Probe CAMEBAX SU-30 microprobe in the Electronic Microscopy Laboratory of the Department of Geology, University of Chile. Elements were measured using wavelength dispersion spectrometry (WDS), with an acceleration voltage of 15 kV, an electric current of 10 nA for silicates and 20 nA for oxides, and a counting time of 10 s for both. The energy beam was focused to a 2 μm size point (mode fix) or in scanner mode with 20,000 times magnification (~30 μm$^2$). Standards for silicates were wollastonite, ortoclase, diopside, albite, rodonite, rutile, and andradite; and for oxides, periclase, corundum, rutile, hematite (specular), chrome oxide, nickel oxide, and cassiterite. Quantitative analysis in silicates and oxides were carried out using XMAS 7.0 software; silicates and oxides were corrected using the PAP algorithm (Puochou and Pichoir, 1984) and ZAF algorithm, respectively. Biotites were classified using ternary diagrams (Beane, 1974) and the magnetic mineralogy classification was conducted using the ILMAT Excel application (Lepage, 2003) and ternary diagrams (O'Reilly, 1984).

**Table 1**
Site, lithology, geologic unit or formation, location, *in-situ* magnetic intensity (NRM) and susceptibility ($\chi$), and Q ratio from rocks of the Los Pelambres porphyry copper deposit (sites LP01–LP08) and the greater Los Pelambres regional outcrops (sites IL10, IL15–IL27, and LP09–LP14).

| | number of samples | Site | Lithology | Unit | UTM N | UTM E | NRM ($A \cdot m^{-1}$) | $\chi$ (S.I.) | Q |
|---|---|---|---|---|---|---|---|---|---|
| Los Pelambres deposit | 1 | LP01 | Intrusive | Los Pelambres Mine Quartzdiorite | 6,490,515 | 358,869 | 0.208 | 0.0009 | **15** |
| | 2 | LP02 | Intrusive | Los Pelambres Mine Igneous Breccia | 6,489,901 | 358,757 | 0.182 | 0.0004 | **31** |
| | 3 | LP03 | Intrusive | Los Pelambres Mine Hydrothermal Breccia | 6,489,836 | 358,989 | 0.107 | 0.0062 | 1.1 |
| | 4 | LP04 | Intrusive | Los Pelambres Mine Quartzdiorite | 6,490,859 | 358,490 | – | – | – |
| | 5 | LP05 | Intrusive | Los Pelambres Mine Igneous Breccia | 6,491,089 | 358,932 | 0.011 | 0.0007 | 0.94 |
| | 6 | LP06 | Intrusive | Los Pelambres Mine Quartzdiorite | 6,491,222 | 359,409 | 0.263 | 0.0003 | **56** |
| | 7 | LP07 | Intrusive | Los Pelambres Mine Quartzdiorite | 6,490,613 | 359,618 | 0.115 | 0.0185 | 0.38 |
| | 8 | LP08 | Intrusive | Los Pelambres Mine Quartzdiorite | 6,490,290 | 358,130 | 0.002 | 0.0020 | 0.06 |
| The greater Los Pelambres region | 1 | IL10 | Intrusive | Illapel Superunit | 6,468,205 | 296,746 | 0.474 | 0.0408 | 0.71 |
| | 2 | IL15 | Intrusive | Illapel Superunit | 6,482,665 | 307,920 | 0.145 | 0.0532 | 0.17 |
| | 3 | IL16 | Intrusive | Illapel Superunit | 6,488,726 | 299,121 | 0.021 | 0.0014 | 0.88 |
| | 4 | IL17 | Intrusive | Illapel Superunit | 6,491,540 | 296,642 | 0.223 | 0.0218 | 0.62 |
| | 5 | IL18 | Intrusive | Illapel Superunit | 6,497,747 | 296,815 | 0.115 | 0.0162 | 0.43 |
| | 6 | IL19 | Intrusive | Cogotí Superunit | 6,470,620 | 342,265 | 0.042 | 0.0059 | 0.43 |
| | 7 | IL20 | Intrusive | Cogotí Superunit | 6,470,618 | 342,131 | 0.057 | 0.0078 | 0.44 |
| | 8 | IL21 | Intrusive | Cogotí Superunit | 6,469,895 | 332,671 | 0.868 | 0.0793 | 0.67 |
| | 9 | IL23 | Intrusive | Illapel Superunit | 6,478,148 | 320,055 | 0.094 | 0.0326 | 0.18 |
| | 10 | IL24 | Intrusive | Illapel Superunit | 6,486,504 | 316,331 | 0.169 | 0.0401 | 0.26 |
| | 11 | IL25 | Intrusive | Illapel Superunit | 6,511,894 | 300,815 | 0.319 | 0.0348 | 0.56 |
| | 12 | IL27 | Intrusive | Illapel Superunit | 6,517,936 | 290,734 | 0.524 | 0.0856 | 0.37 |
| | 13 | LP11 | Intrusive | Cogotí Superunit | 6,513,358 | 329,292 | 0.247 | 0.0651 | 0.23 |
| | 14 | LP09 | Andesite | Los Pelambres Formation | 6,481,732 | 354,419 | 0.401 | 0.0392 | 0.63 |
| | 15 | LP10 | Andesite | Viñitas Formation (upper member) | 6,479,913 | 351,730 | 0.291 | 0.0346 | 0.51 |
| | 16 | LP12 | Andesite | Viñitas Formation (upper member) | 6,511,672 | 327,289 | 0.123 | 0.0288 | 0.26 |
| | 17 | LP13 | Red sandstone | Viñitas Formation (lower member) | 6,507,483 | 325,393 | 0.005 | 0.0002 | 1.6 |
| | 18 | LP14 | Red siltstone | Quebrada Marquesa Formation | 6,505,310 | 319,214 | 0.045 | 0.0008 | 3.4 |
| | 19 | IL22 | Red siltstone | Quebrada Marquesa Formation | 6,470,860 | 328,776 | 0.016 | 0.0001 | 7.7 |

Bold values indicate significance at Q ratios higher than 10.

### 3.3. Paleomagnetic techniques

The paleomagnetic properties of rocks were measured for all collected samples at the laboratory of Paleomagnetism in the Department of Geology, University of Chile (Institut de recherche pour le développement-IRD donation).

All samples were thermally demagnetized (11 steps; 150, 210, 260, 310, 360, 410, 460, 510, 560, 610, 640, 700 °C) in a TD-48 ASC Scientific Oven. Magnetic susceptibility ($\chi$) was measured on the paleomagnetic mini-cores (standard 2.5 cm diameter and 2.2 cm long) with a Bartington MS2 susceptibility meter after each step to control magnetic mineralogical changes upon heating. Demagnetization process was measured with a JR5A (range $10^{-5}$–1500 $A \cdot m^{-1}$) spinner magnetometer. Magnetic mineralogy was investigated by means of variations of low-field magnetic susceptibility versus temperature (K-T experiments) in a high sensibility susceptibility meter (KLY-3 Kappabridge Pick-up Unit) with a temperature control unit for Magnetic Susceptibility-Temperature Variation (AGICO, Advanced Geoscience Instrumental Company, model CS-3); warming and cooling cycles were carried out between 22 and 700 °C under open air conditions, which favored mineral oxidation reactions during the process. Characteristic remanent magnetization (ChRM) component directions were determined using principal component analysis (Kirschvink, 1980). Site mean directions were defined using classical Fisher statistics or a combination of best fit lines and remagnetization circles when necessary (McFadden and McElhinny, 1988). Additionally, the Koenisberger ratio "Q" (Table 1 and Eq. (1)) was determined to establish zones where the induced magnetic signal ($Q < 1$) or the remanent magnetic signal is dominant ($Q \geq 1$).

Eq. (1). Koenisberger ratio. IM corresponds to the induced magnetization; MF corresponds to the magnetic field (obtained using StereoOSX software).

$$Q = NRM \cdot IM \rightarrow IM = \chi \cdot MF \quad (1)$$

## 4. Results

### 4.1. Alteration silicates and magnetic minerals of the Los Pelambres porphyry copper deposit

The observation and characterization of alteration and magnetic minerals were performed in samples from sites LP01 to LP08 (Fig. 1c) as explained in the following paragraphs.

Hand samples of sites LP01 and LP02 (located in the central and deepest part of the pit; Fig. 1c) appeared unaltered. Primary mafic minerals of the Los Pelambres deposit were classified by Atkinson et al. (1996) as hornblende and magmatic biotites, and despite the fact that samples of these sites appeared unaltered, microprobe analysis of these minerals (Fig. 2a and b) and subsequent classification in Beane's ternary diagram (Fig. 2g) revealed that mafic minerals correspond to alteration biotites, indicating the presence of potassic alteration. In addition, these samples present overprinted phlogopites, sericite, and quartz. These alteration minerals indicate two separate alteration stages: selective biotitization of pre-existent mafic minerals and a superimposed phyllic alteration. Observed ore minerals at these sites correspond to chalcopyrite, bornite, chalcocite, and covellite, along with Fe-Ti oxides (Fig. 3a and b). At site LP01, these oxides of 300 μm average diameter show variable contents of $TiO_2$ (detection limit-DL to 17 wt%) and $Fe_2O_{3total}$ (80 to 100 wt%; Fig. 3a). Oxides from site LP02 are similar to those from LP01 with a maximum size of 400 μm, and are anhedral and contain apatite inclusions (Fig. 3b). Compositionally these are characterized by $TiO_2$ content in the range of 16 to 20 wt% and $Fe_2O_{3total}$ in the range of 78 to 90%. Both sites show rutile exsolution textures (Fig. 3a and b) and are spatially and likely genetically related to biotites (Fig. 2a and b). The composition of the oxides at both sites, LP01 and LP02, fits well into the titano-hematites solid solution series classification (Fig. 3i).

Rocks from site LP03 (located in the south central part of the pit; Fig. 1c) correspond to diorites and tonalites of porphyritic texture.

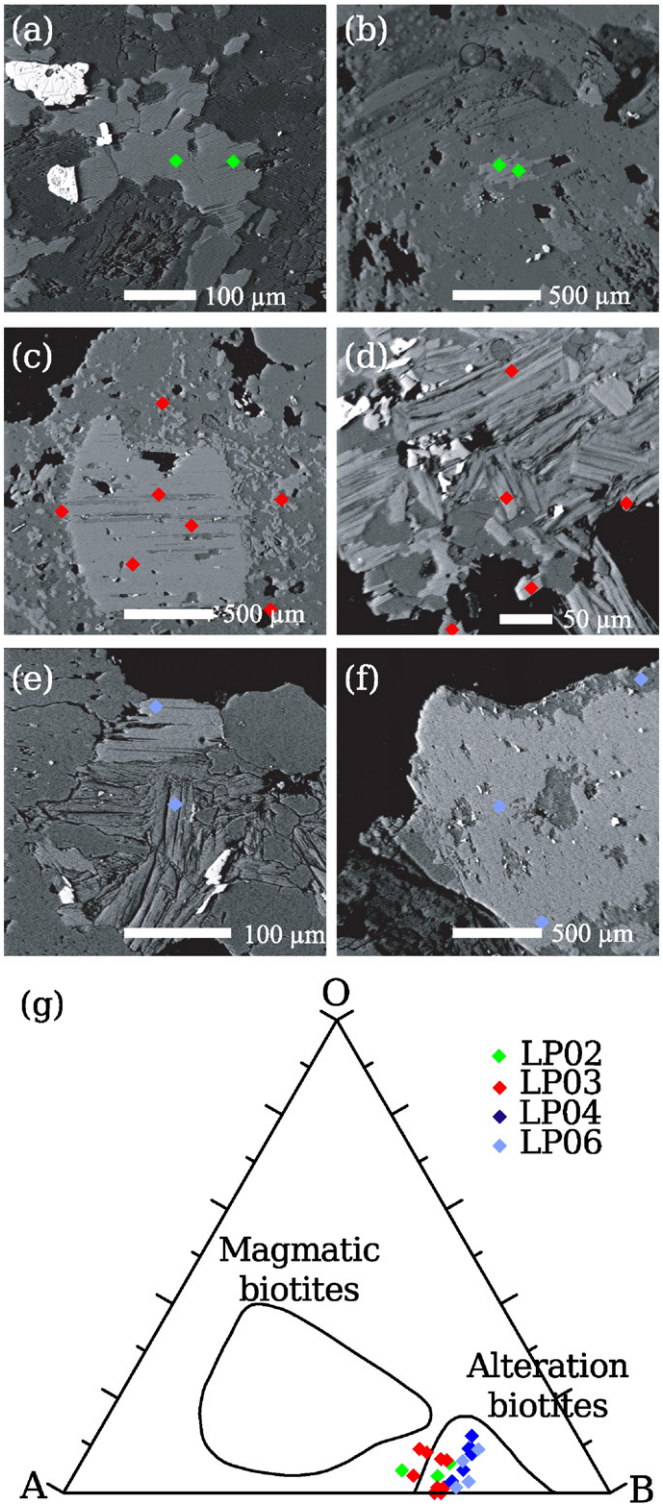


**Fig. 2.** Scanning electron photomicrographs of alteration biotites of the Los Pelambres porphyry copper deposit. (a and b) Site LP02; (c and d) Site LP03; (e and f) Site LP06; (g) Biotite classification ternary diagram (Beane, 1974) where O is proton deficient oxyannite, A is annite, and B is phlogopite.

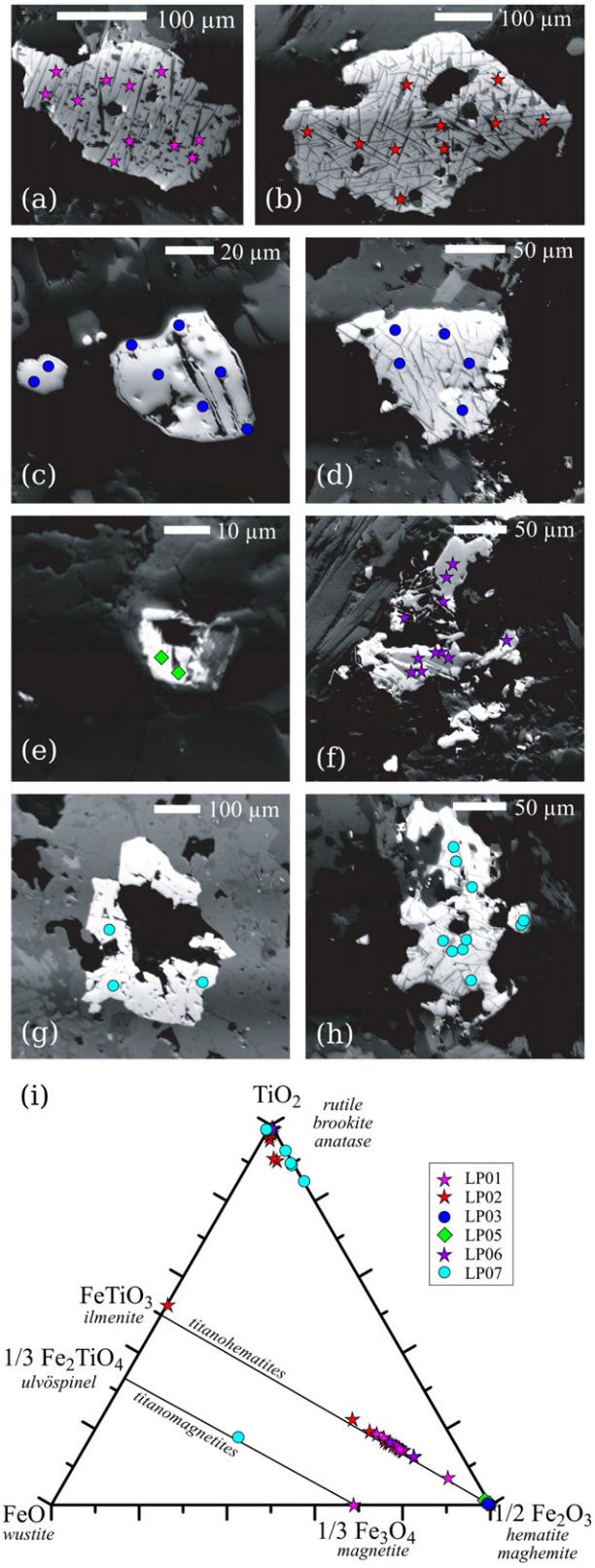


**Fig. 3.** Scanning electron photomicrographs of magnetic minerals of the Los Pelambres porphyry copper deposit. (a) Site LP01; (b) Site LP02; (c and d) Site LP03; (e) Site LP05; (f) Site LP06; (g and h) Site LP07; (i) Ternary diagram of the titano-hematite and titano-magnetite classifications (O'Reilly, 1984).

Thin sections show zoned and sericitized plagioclase phenocryst. As in sites LP01 and LP02, microprobe results indicate that the biotite (Fig. 2c and d) composition is related to the re-equilibrium of altered pre-existent mafic minerals or to a transitional alteration zone (Fig. 2g). These rocks also contain phlogopites and phengites. Alteration mineral associations distinguish four alteration events: non-selective biotitization, moderate phyllic alteration, and weak argillic and chloritic alterations. Ore minerals associated with Fe-Ti oxides described within this site are bornite, covellite, and chalcopyrite. Dimensions of analyzed oxides from this site are less than 100 μm diameter, are anhedral, and

some exhibit dark rims (Fig. 3c) and others show exsolution textures (Fig. 3d). Compositionally there are two groups of oxides, one constituted by $Fe_2O_{3total} \pm SiO_2 \pm Al_2O_3 \pm TiO_2$ (Fig. 3c) and others composed of $Fe_2O_{3total} \pm TiO_2$ (Fig. 3d). For the first group, total oxides are not close to 100% due to the lack of standard samples for $Al_2O_3$ and $SiO_2$ during the oxide analysis by microprobe, yet $Fe_2O_{3total}$ ranges between 82 and 99 wt%, and $TiO_2$ between DL and 0.2 wt%. These oxides are classified as magnetites (Fig. 3i). The second group shows $TiO_2$ in the range of 14 to 17 wt% and $Fe_2O_{3total}$ in the range 76 to 80 wt%. These minerals are classified as titano-hematites (Fig. 3i), but in contrast to other sites, exsolution textures do not correspond to pure rutile (19 to 29 wt% $Fe_2O_{3total}$), but are closer to a pseudobrookite composition.

Rocks of site LP04 (northwestern side of the pit; Fig. 1c) correspond to metamorphosed andesites. Main alteration minerals here are biotite, chlorite, and to a lesser extent quartz (in veinlets). As in the previously described sites, biotite microprobe analysis shows that mafic minerals correspond to alteration biotites (Fig. 2g). The alteration mineralogy differentiates two main alteration events: an intense biotitization and weak chloritization. Metallic minerals at this site correspond only to pyrite and Fe-Ti oxides (not shown in Fig. 3).

Rocks of site LP05 (northern limit of the pit; Fig. 1c) show a highly obliterated texture with intense phyllic and argillic alterations. Plagioclase phenocrysts are only recognizable by their twinning and no mafic minerals were observed. Ore mineralogy is composed of chalcopyrite, bornite, and covellite, in association with pyrite and subordinated Fe-Ti oxides (Fig. 3e). These oxides are characterized by 20 μm average-sized subhedral borders, and are scarce and disseminated within a quartzitic groundmass. No exsolution textures are observed within these oxides (Fig. 3e). The composition of oxides at this site is mainly $Fe_2O_{3total}$ (87 to 95 wt%), and the oxides are classified as hematite using the ILMAT application (Lepage, 2003) and ternary diagrams of O'Reilly (1984); Fig. 3i).

At LP06 site (located in the north-eastern border of the pit; Fig. 1c), plagioclase is the primary mineral, and alteration minerals correspond mainly to biotite, quartz, sericite, and to a lesser extent clays and phlogopite. Microprobe analysis of mafic minerals (Fig. 2e and f) classify these as alteration biotites (Fig. 2g). Secondary minerals distinguish two main alteration stages for this site: selective biotitization of pre-existent mafic minerals and superimposed phyllic alteration. Observed ore minerals are chalcopyrite, covellite, and molybdenite. In addition, Fe-Ti oxides are present in a relatively high proportion (~1.5%; Fig. 3f). These oxides have a maximum diameter of 70 μm, are anhedral and exhibit exsolution textures. The composition of the oxides ranges between 79 to 83 wt% $Fe_2O_{3total}$ and 12 to 15 wt% $TiO_2$. Exsolution textures are constituted by rutile (98 to 100 wt% $TiO_2$). These oxides are classified as titano-hematites (Fig. 3i).

In the LP07 site (eastern zone of the pit, north of La Virgen hill; Fig. 1c), primary minerals correspond only to plagioclase phenocrysts. Alteration minerals are characterized by moderate amounts of secondary biotite and quartz, and to a lesser extent by sericite and chlorite. Biotitization is non-selective (no chemical analyses were performed on samples of this site). Ore minerals are bornite, chalcopyrite, chalcocite, and covellite; Fe-Ti oxides are also present (~1%; Fig. 3g and h). Oxides from this site are similar to those found at LP03, having two distinct groups of minerals. On the one hand, anhedral 200 μm average size oxides with no exsolution textures (Fig. 3g), composed mainly of $Fe_2O_{3total}$ ($TiO_2$ ranges between DL and 0.06 wt%), are classified as magnetites (Fig. 3i). Conversely, anhedral 100 μm average size oxides with exsolution textures (Fig. 3h), composed by $Fe_2O_{3total}$ (85 to 89 wt%) and $TiO_2$ (16 to 17 wt%), correspond to titano-hematites (Fig. 3i). Exsolution textures are constituted by $TiO_2$ ($95 \geq TiO_2 \geq 87$ wt%) and $Fe_2O_{3total}$ ($16 \geq Fe_2O_{3total} \geq 2$ wt%), signifying the presence of rutile with minor changes in the cationic number of its structural formula.

Rocks at the LP08 site (western area of the pit; Fig. 1c) are not discernible, yet according to previous mapping these are located in the limit of andesites and quartz-diorites (Perelló et al., 2012; Fig. 1c). The primary mineralogy is completely obliterated and alteration minerals (in decreasing order) correspond to sericite, quartz, clays, tourmaline, and pyrophyllite; these are described by an intense phyllic alteration stage overprinted by a moderate argillic alteration. Ore mineralogy corresponds to chalcopyrite, which is present with pyrite (~4%) and Fe-Ti oxides (not shown in Fig. 3).

### 4.2. Magnetic properties of rocks of the Los Pelambres porphyry copper deposit

Magnetic properties, susceptibility, intensity of remanence, curie temperatures, and demagnetization directions in the Los Pelambres mine were characterized at the same sites as described in the previous section.

Site LP01 shows an *in-situ* NRM intensity of 0.208 $A \cdot m^{-1}$, average $\chi$ of 0.000815 S.I., and Q ratio values over 10 (Table 1). During the heating process, some samples at this site increase $\chi$ at 410 °C (Fig. 4a). Magnetic intensity decreases constantly during the heating process, and magnetization loss occurs between the range of 570–630 °C (Fig. 5a). K-T experiments show flat curves until 400 °C followed by a steady increase until 570–580 °C, which could be due to newly formed magnetic minerals from pre-existent sulfides by oxidation in the thermocouple (Fig. 6a). The vector plot is directed to the origin presenting unblocking temperatures over 560 °C (Fig. 7a).

For site LP02, the *in-situ* average intensity is 0.182 $A \cdot m^{-1}$, average $\chi$ is 0.000359 S.I., and Q ratio is 31 (Table 1). During heating, samples from this site show an increase of $\chi$ at nearly 400 °C (as site LP01; Fig. 4b). Magnetic intensity shows unblocking temperatures that fall between 570 and 610 °C (Fig. 5a). K-T curves are similar to those performed on samples from site LP01, with a flat pattern until 400 °C and a sustained increase thereafter (Fig. 6b). The vector plot is directed to the origin with unblocking temperatures over 560 °C (Fig. 7b).

At site LP03, the *in-situ* average magnetic intensity is 0.107 $A \cdot m^{-1}$, average $\chi$ value is 0.00616 S.I., and Q ratio is 1.1 (Table 1). During the heating process, $\chi$ decreases constantly (Fig. 4c), and samples are demagnetized at 590–610 °C (Fig. 5a). K-T experiments show a flat curve until 350 °C, and all magnetization is lost at nearly 580 °C (Fig. 6c). Vector plots are directed to the origin with unblocking temperatures over 560 °C (Fig. 7c).

Site LP04 was not measured because of the metamorphism that affected these rocks coupled with the intense hydrothermal alteration that prevented the respective proper measurements.

Site LP05 exhibits an *in-situ* average magnetic intensity of 0.0111 $A \cdot m^{-1}$, average $\chi$ of 0.000722 S.I., and Q ratio of 0.9 (Table 1). During heating, these samples show different behaviors related to magnetic $\chi$ and intensity (Fig. 4d and Fig. 5b, respectively). K-T curves show two decreases, one at approximately 270 °C and the other at nearly 570 °C (Fig. 6d). Vector plots are directed to the origin and are over 560 °C (Fig. 7d).

At site LP06, magnetic properties are similar to sites LP01 and LP02. *In-situ* average magnetic intensity is 0.263 $A \cdot m^{-1}$, average $\chi$ is 0.000287 S.I., and Q ratio is the highest of all sites (Table 1). Throughout the demagnetization process, $\chi$ increases at nearly 400 °C (similar to sites LP01 and LP02; Fig. 4e) and magnetic intensity is relatively constant until 600 °C, where samples lose all magnetization (Fig. 5a). K-T curves for this site exhibit flat patterns with a slight decrease at ~350 °C (Fig. 6e), which might be interpreted as destruction of maghemite (Astudillo et al., 2008; Krása and Herrero-Bervera, 2005; Riveros et al., 2014; Townley et al., 2007). The vector plot is directed to the origin with unblocking temperatures over 560 °C (Fig. 7e).

For site LP07, the *in-situ* average magnetic intensity is 0.115 $A \cdot m^{-1}$, average $\chi$ is 0.0185 S.I., and Q ratio is 0.38 (Table 1). These samples systematically lose $\chi$ (Fig. 4f) and magnetization, exhibiting two unblocking temperatures at 570 °C and 600 °C (Fig. 5a). Susceptibility versus high temperature experiments show a nearly flat curve, where

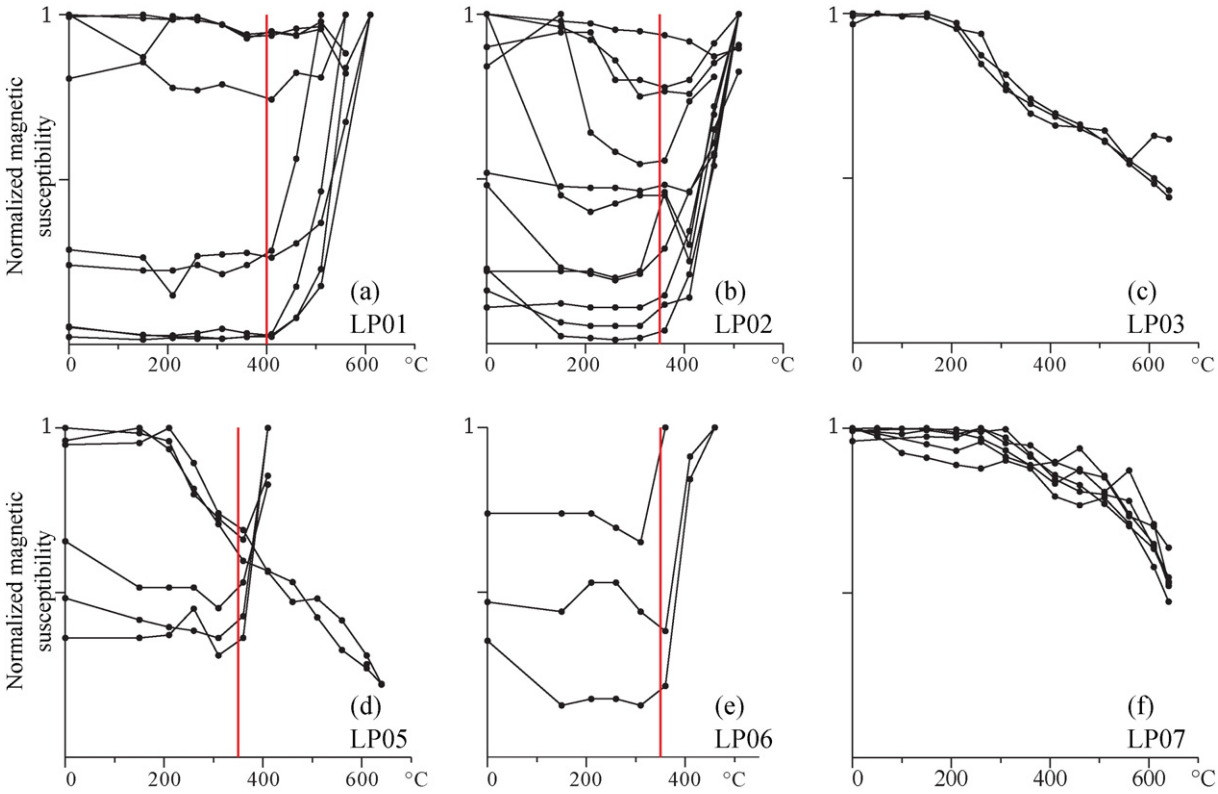


**Fig. 4.** Normalized magnetic susceptibility *vs.* temperature (°C). (a) Site LP01; (b) Site LP02; (c) Site LP03; (d) Site LP05; (e) Site LP06; (f) Site LP07. The red line for each site indicates the heating curve of various samples.

it was only possible to observe a change at 380 °C (not shown in Fig. 6). For this site, the vector plot was directed to the origin, with unblocking temperatures close to 560 °C (Fig. 7f).

Analysis for site LP08 are only *in-situ* and within the first stages of demagnetization due to the intense alteration present in these samples. *In-situ* values are 0.00195 $A \cdot m^{-1}$ for magnetic intensity, 0.00195 S.I. for $\chi$, and Q rates are the lowest in the mine and at the outcrops of the zone (0.06; Table 1). During cooling, the susceptibility versus high temperature curve displays a positive irreversibility for these samples; this could be due to the important presence of iron sulfides at this site (pyrite), which in an oxygenated environment were transformed into iron oxides during heating (Fig. 6f).

### *4.3. Magnetic properties and magnetic minerals of intrusive rocks within the greater Los Pelambres region*

Results for intrusive rocks within the greater Los Pelambres region are presented in this section since mineralization in this deposit is related to the intrusives.

The analysis of unaltered magnetic minerals of intrusive rocks from the Illapel Superunit (IL16, Figs. 1b and 8a–c) and the Cogotí Superunit (IL20, Figs. 1b and 8d–f) indicate that these minerals are 200 to 500 μm in size, are subhedral to anhedral, and present irregular rims. Compositionally these minerals contain $Fe_2O_{3total}$ in the range 77 to 100 wt%. Samples with minor contents of $Fe_2O_{3total}$ exhibit Al, Si, and

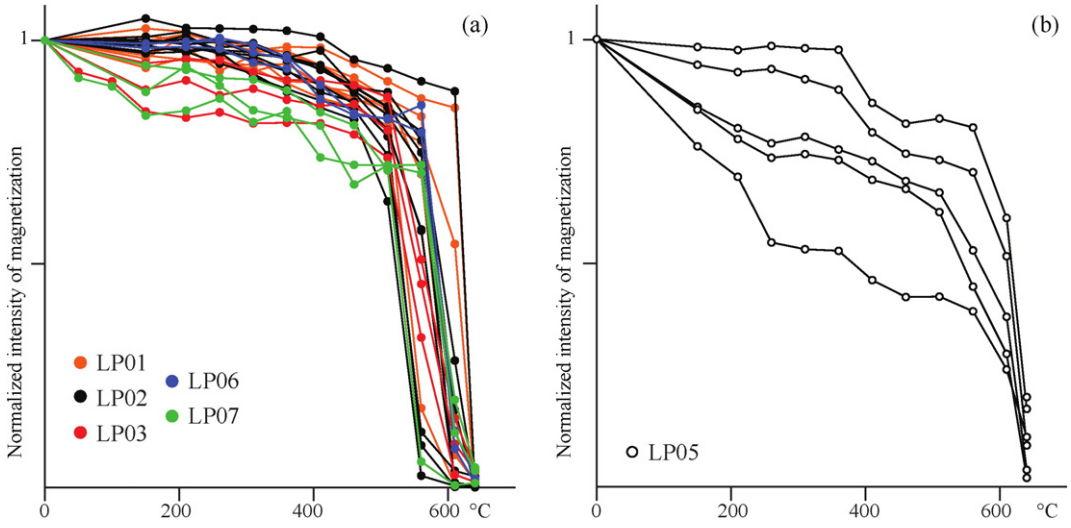


**Fig. 5.** Normalized intensity of magnetization *vs.* temperature (°C). (a) Sites LP01, LP02, LP03, LP06, LP07; (b) Site LP05.

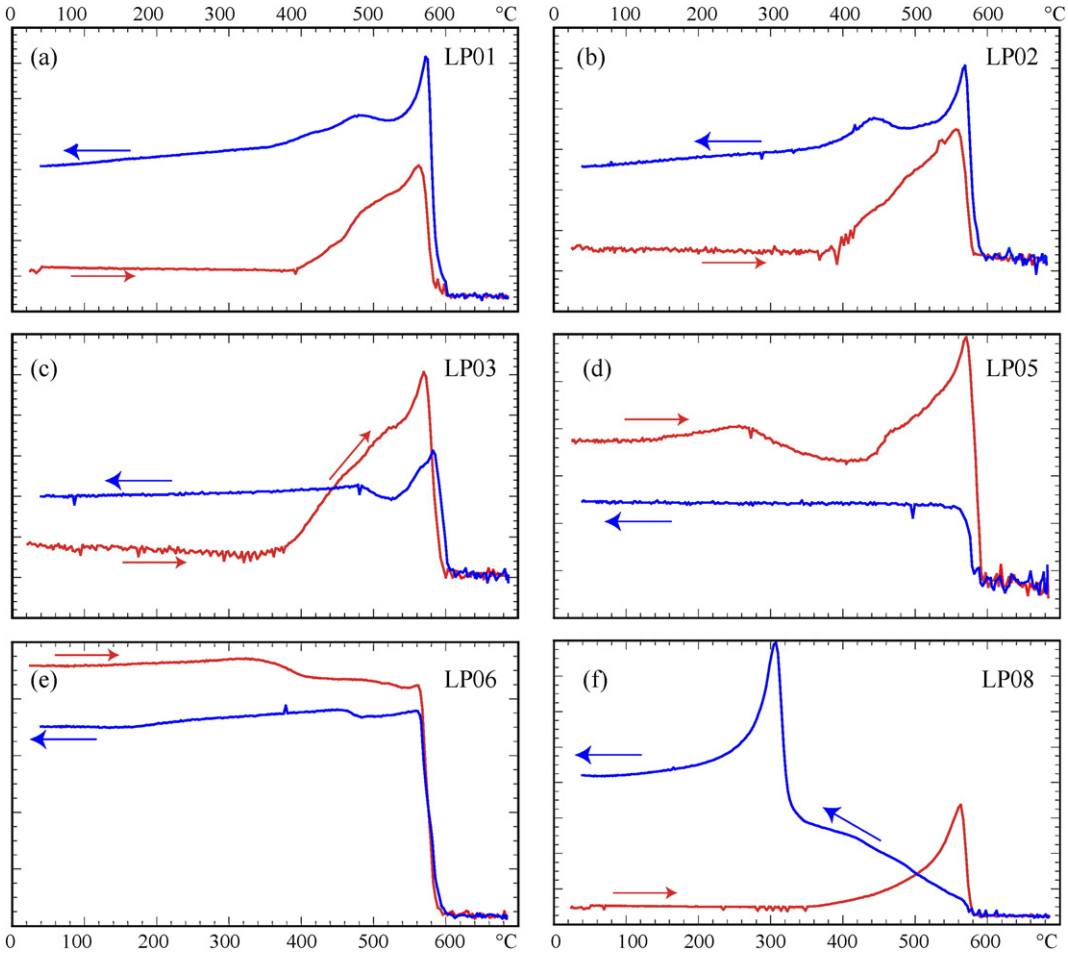


**Fig. 6.** K-T curves. (a) Site LP01; (b) Site LP02; (c) Site LP03; (d) Site LP05; (e) Site LP06; (f) Site LP08. Right and left arrows indicate the heating (normal, red) and cooling (inverse, blue) processes, respectively.

Ti; $TiO_2$ concentrations range between DL and 9.4 wt%, however Al and Si were not analyzed quantitatively. The main difference when comparing oxides of igneous rocks from the greater Los Pelambres region (Fig. 8) to oxides of Los Pelambres mine (Fig. 3) is the lack of clear exsolution textures.

In relation to magnetic properties, Cretaceous intrusive rocks exhibit the highest values for magnetic intensity and susceptibility (Illapel Superunit). Curie temperatures of most intrusive rocks range between 550 and 600 °C. This range of temperatures plus magnetic intensity and susceptibility suggest the presence of magnetic minerals of the titano-magnetite solid solution series as main magnetization carriers.

## 5. Discussion

### *5.1. Hydrothermal alterations, ferromagnetic mineral transformations, and implications for copper mineralization*

Experimental ternary stability diagrams indicate that rutile can be stable and present with titano-hematites at temperatures of approximately 600 °C (Lindsley, 1991). In the Los Pelambres porphyry copper deposit, the hydrothermal alteration temperature for green mica and Type 4 veinlets (younger veins in the deposit) are calculated at approximately 550 °C (Skewes and Atkinson, 1985). Green mica veinlets are rare and do not have an important association with copper mineralization. Conversely, Type 4 veins host important amounts of copper sulfides, containing up to 80% in portions of the deposit (Vehrs and Staff, 1982).

High temperature oxidized hydrothermal fluids may transport copper as stable chlorine-rich complex molecules (Richards, 2011). Water-rock interactions, oxidation of pre-existent mafic minerals such as hornblende and magmatic biotites in this deposit (Atkinson et al., 1996; Perelló et al., 2012; Section 4.1), and Fe-Ti oxides of the titano-magnetite series (Fig. 8; Section 4.3) cause a reduction process and transformation of pre-existent mafic minerals to altered biotite (Fig. 2) as well as ferric oxides to titano-hematite and rutile (Fig. 3). Oxidation processes of the host rock (Corbett and Leach, 1998; Pollard, 2006; Reed, 1997) coupled with the cooling of hydrothermal fluids below 400 °C (Hezarkhani et al., 1999; Klemm et al., 2007; Landtwing et al., 2005; Ulrich et al., 2001) provide mechanisms for Cu precipitation. Hydrothermal fluids associated with potassic alteration oxidize ferric iron-bearing minerals (Pollard, 2006; Reed, 1997) and the hydrothermal fluid is effectively reduced to the chalcopyrite-bornite-magnetite stability field (Reed, 1997). This implies that the oxidizing hydrothermal fluid could have played an important role in Cu mineralization within this deposit.

### *5.2. Lithology, alteration, and magnetic groups of the Los Pelambres porphyry copper deposit*

Field and laboratory results of this study discern three lithologic-alteration groups in the Los Pelambres porphyry copper deposit. Rocks within each group share similar alteration and magnetic properties in addition to hosting comparable ferromagnetic minerals.

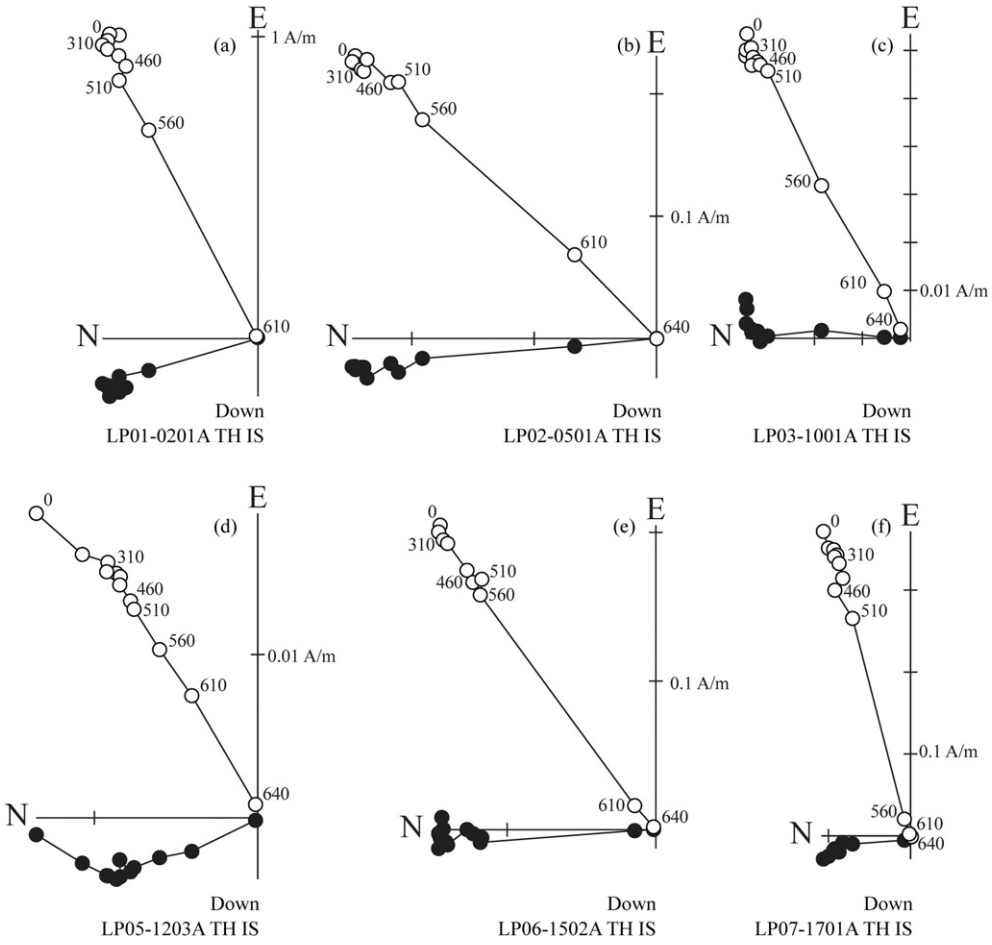


**Fig. 7.** Demagnetization zijderveld diagrams (Kirschvink, 1980; McFadden and McElhinny, 1988). (a) Site LP01; (b) Site LP02; (c) Site LP03; (d) Site LP05; (e) Site LP06; (f) Site LP07.

*5.2.1. High magnetic remanence group (HMRG; LP01, LP02 and LP06 sites)*

Rocks included within this group are represented by tonalitic and dioritic porphyries affected by selective biotitization, overprinted by quartz-sericite hydrothermal alteration (potassic and phyllic). These rocks present Q ratios ≥10 (Table 1) indicating that the magnetic signal is given by remanent magnetism (Alva-Valdivia and López-Loera, 2011; Alva-Valdivia and Urrutia-Fucugauchi, 1998; McEnroe et al., 2001). The demagnetization process shows that the principal magnetic signal for HMRG is due to titano-hematite solid solution series minerals with exsolution textures composed of rutile (Figs. 3a–f). Such textures and exsolution of rutile represents a clear feature of hydrothermal alteration, in particular for potassic alteration, implying that the magnetic properties of these rocks are likely the result of hydrothermal alteration and mineralization processes, overprinted on the original host rock.

*5.2.2. High magnetic susceptibility group (HMSG; LP03 and LP07 sites)*

Rocks included within this group are porphyritic diorites with non-selective biotitic and quartz-sericite alteration. For *in-situ* magnetic properties, these rocks show variable $\chi$ values, relatively constant NRM values, and Q ratios close to 1 (Table 1). Two different ferromagnetic minerals are present in the HMSG: (i) titano-magnetites with Al-Si-Ti reaction rims, but no exsolution textures (Fig. 3c and g), and (ii) titano-hematites with exsolution textures composed of rutile (as in HRMG; Fig. 3d and h). Some samples of this group show unstable magnetic properties and all show low Q ratios; these characteristics are usually associated with multidomain magnetite grains (Alva-Valdivia et al., 2003a; Astudillo et al., 2008), suggesting that the HMSG magnetic signal was likely acquired during hydrothermal alteration and is given by multidomain titano-magnetites. Rutile exsolution also evidences hydrothermal alteration processes.

*5.2.3. Low magnetic susceptibility/low NRM group (LMSG; LP05)*

Rocks included within this group present pervasive argillic alteration and intense quartz-sericite (phyllic) alteration, the original primary mineralogy is not discernible. *In-situ* magnetic properties for these rocks show on average low $\chi$ and moderate to low NRM values, with a Q ratio lower than 1 (Table 1), implying that the magnetic signal could be given by an acquired magnetization during the hydrothermal alteration. The weak magnetic signal results of LMSG are given by rare and small (20 μm average) hematite species with no noticeable exsolution textures (Fig. 3e).

*5.3. In-situ magnetic properties as an indicator for prospective porphyry copper deposits*

*5.3.1. Magnetic properties of hydrothermally altered rocks in contrast to the surrounding country rocks*

Studied country rocks in the region of Los Pelambres are conformed by stratified Cretaceous volcanic and sedimentary rocks of Los Pelambres, Quebrada Marquesa, and Viñitas Formations, and by Lower Cretaceous intrusive rocks of the Illapel Superunit and Upper Cretaceous to Tertiary intrusive rocks of the Cogotí Superunit (Table 1). Most data from unaltered country rocks show a near-linear relationship between $\chi$ and NRM (Fig. 9a).

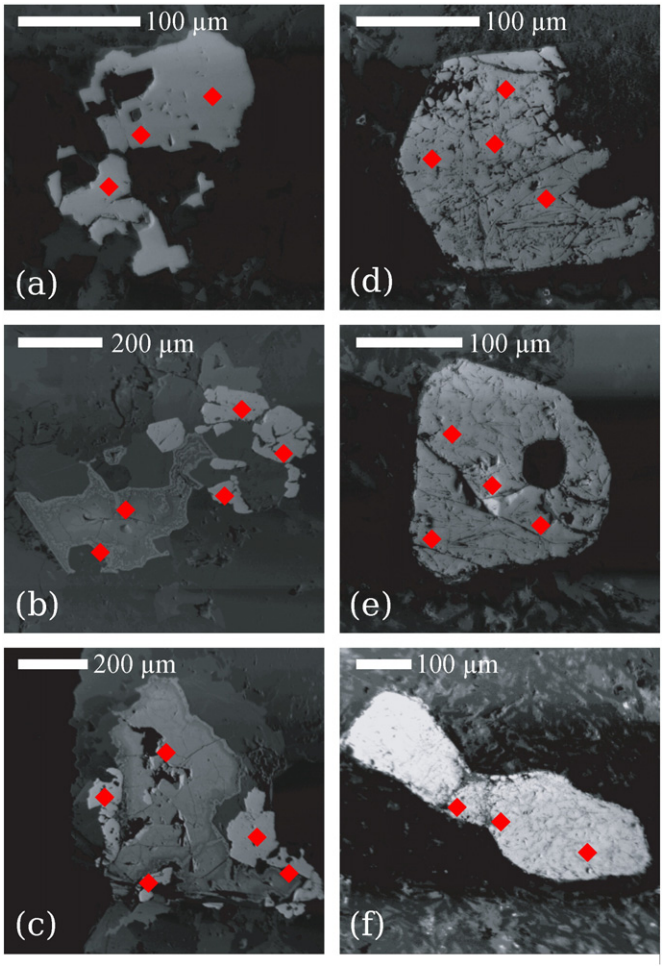


**Fig. 8.** Scanning electron photomicrographs of magnetic minerals of the greater Los Pelambres region. (a, b, and c) Magnetic minerals of the Illapel Superunit (IL16; Fig. 1b). (d, e, and f) Magnetic minerals of the Cogotí Superunit (IL20; Fig. 1b).

*In-situ* magnetic properties of rocks from the HMSG and LMSG groups within the deposit are comparable to the regional intrusive and andesitic rocks within a similar linear trend, with Q ratios close to 1 (Table 1). Rocks from the HMRG group are markedly distinct from all others, deviating from the linear trend (Fig. 9a). These distinct *in-situ* magnetic properties are either the result of the modification of the original properties of rocks or the result of newly crystallized ferromagnetic minerals during hydrothermal alteration. For instance, intrusive rocks of the Illapel and Cogotí Superunits host titano-magnetite as the prime magnetic carrier without clear evidence of rutile exsolution textures (Fig. 8). In contrast, intrusive rocks in the Los Pelambres porphyry copper deposit owe their *in-situ* magnetic and paleomagnetic properties mostly to titano-magnetite or titano-hematite (Fig. 3), depending on lithology-alteration properties.

*5.3.2. In-situ magnetic properties of Chilean porphyry copper deposits*

To expand on the practical relevance of this study regarding the exploration of porphyry copper deposits, *in-situ* NRM and $\chi$ data of altered intrusive rocks from various deposits in Chile (Chuquicamata, El Teniente, and Los Pelambres) were compared in Fig. 9b. These deposits are relatively small in comparison to regional-scale geologic units; the area of Chuquicamata is approximately 4.8 km$^2$, (estimated from Ossandón et al., 2001), El Teniente is approximately 1 km$^2$ (estimated from Astudillo et al., 2010), and the initial Los Pelambres intrusion is less than 11 km$^2$ (Perelló et al., 2012). Neighboring regional intrusions such as the Illapel and Cogotí Superunits are greater than 1800 km$^2$ and 300 km$^2$, respectively (Fig. 1b). It is important to note the high variability in the data while considering the small surface area of these deposits in comparison to the regional superunits.

All porphyry copper deposit sampling sites characterized by alteration type or alteration mineralogy were plotted as well (Fig. 9b). In Fig. 9b there is an apparent clustering of data when alteration and *in-situ* magnetic properties are plotted together. Phyllic and pervasive alterations generally are characterized by low NRM values (Fig. 9b), which could be explained by the fact that magnetite is not stable in phyllic alteration environments (Corbett and Leach, 1998; Reed, 1997; Sillitoe, 2010). Chloritic alteration is mostly associated with intermediate NRM values (Fig. 9b) because magmatic and hydrothermal magnetite is transformed to hematite (martite or specularite) as a result of this type of alteration (Sillitoe, 2010). Potassic alteration commonly plots in the high NRM field (Fig. 9b). This is supported by the fact that

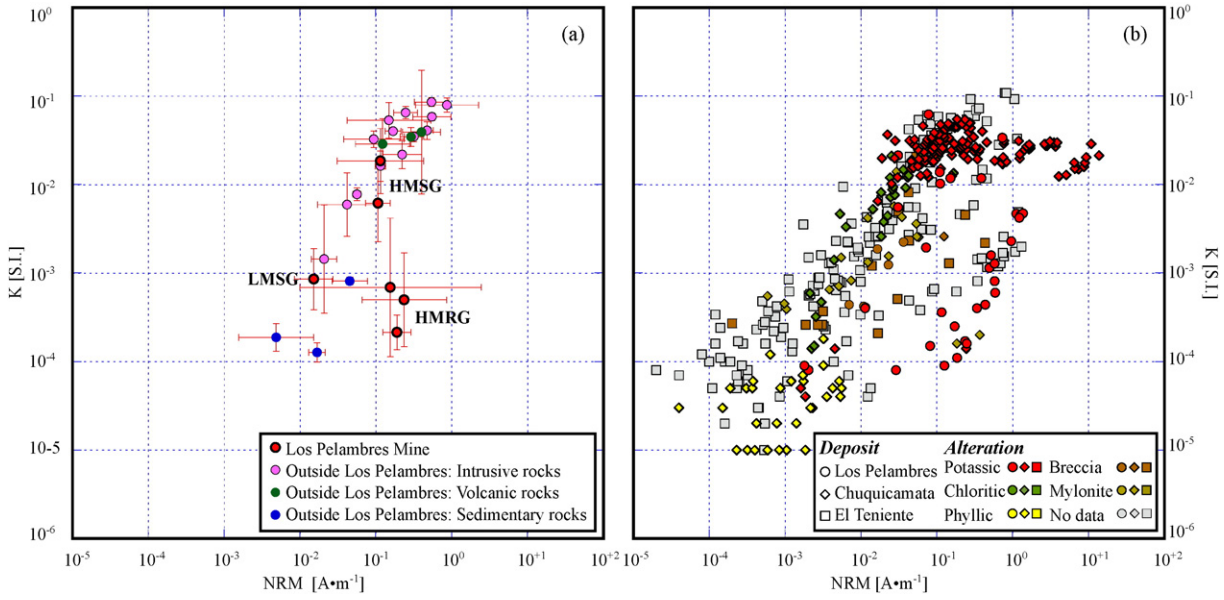


**Fig. 9.** *In-situ* magnetic properties. (a) Rocks from the greater Los Pelambres region and Los Pelambres porphyry copper deposit. Within each site, error bars are shown. (b) Samples from rocks of Los Pelambres, Chuquicamata, and El Teniente porphyry copper deposits; if data is available, alteration type is depicted.

magnetite is a stable mineral under conditions of potassic alteration (Corbett and Leach, 1998; Sillitoe, 2010).

Furthermore, although potassic alteration is characterized by high NRM values in both the Chuquicamata and Los Pelambres porphyry copper deposits, a lower *in-situ* magnetic susceptibility is observed for Los Pelambres. This can be due to the fact that most of the studied samples in this deposit exhibit overimposed phyllic alteration. In addition, this slight difference in magnetic susceptibility might be related to different conditions during formation. Chuquicamata originated between 33 to 36 Ma (Ossandón et al., 2001) from granodioritic rocks of adakitic affinity (highly oxidized, water- and sulfur-rich magma) that would have evolved in a closed or near-closed system (Oyarzun et al., 2014). Los Pelambres on the contrary originated between 13.6 (Perelló et al., 2012) to 12.5 (Bertens et al., 2006) Ma from quartz-diorite intrusions of an adakite-like signature with lower MgO contents as interpreted from slab melt-mantle wedge interactions (Kay et al., 1993; Reich et al., 2003).

### 5.4. What to seek when prospecting?

When considering all rock groups within the Los Pelambres deposit, the *in-situ* magnetic properties vary over a broad range in the NRM, $\chi$, and Q ratios, yet all are within a small data cluster (Fig. 1b and c) when compared to the broad distribution shown in regional samples (Fig. 1b). This would suggest that hydrothermal alteration processes, in particular multi-event stages of alteration and mineralization of dissimilar lithologic host rocks within these deposits, have the overall effect of generating a high paleomagnetic variance when compared to the variance of surrounding country rocks.

Evidence of hydrothermal alteration and recrystallization of ferromagnetic minerals, as a result of fluid-rock reactions and mineral equilibrium, indicate that the original magnetic properties of host and country rocks are in fact modified as a result of the ore rock forming processes. In the case of porphyry copper systems, long lived magmatic-hydrothermal processes will have varying effects on the original magnetic properties of rocks. In fact, some types of hydrothermal alterations may generate singular magnetic properties, in particular those types in which ferromagnetic minerals are stable (e.g., potassic, propylitic, calc-sodic, calc-silicate alterations). The result of magmatic-hydrothermal processes would be expected to modify or generate high short range variance in magnetic properties that are potentially in high contrast to the country rocks. Such concepts are not regularly applied to geophysical exploration (aerial or ground magnetic data processing and interpretation), hence the characteristics of the expected contrasts are not known. The application of these concepts, in addition to the incorporation of regional scale paleomagnetic properties to better interpret magnetic surveys, could be essential to identifying meaningful contrast anomalies which may in fact be related to porphyry copper systems.

In the case of the Los Pelambres porphyry copper system, as shown, the high variability of magnetic data in a small area coupled with the relationship between phyllic and potassic alterations (which show low and high NRM signals respectively) allows us to propose an integrated approach that utilizes field and laboratory methods to measure susceptibility and NRM appropriately. The exploration of porphyry copper deposits by *in-situ* magnetic properties could be associated with a high variability of susceptibility and NRM in smaller, local areas when compared to regional intrusions.

## 6. Conclusions

Results from alteration and magnetic mineralogy coupled with paleomagnetic properties of rocks at the Los Pelambres porphyry copper deposit allow for the following conclusions:

i. In the Los Pelambres deposit, magnetic properties of rocks are carried by titano-hematite and titano-magnetite solid solution minerals, where the former commonly indicates the exsolution of rutile. Magnetic minerals of intrusive rocks from the greater Los Pelambres region show magmatic titano-magnetites and magnetites as the main magnetization carriers.
ii. The oxidizing hydrothermal alteration fluid related to the modification of pre-existent mafic minerals and titano-magnetites to secondary biotite and titano-hematites plus rutile exsolution textures could have played an important role in Cu mineralization of the Los Pelambres porphyry copper deposit.
iii. Paleomagnetic and *in-situ* magnetic properties of rocks within the Los Pelambres deposit may be divided into three groups (HMRG, HMSG, and LMSG). These properties are directly linked to a specific ferromagnetic mineralogy which in turn is related to distinct hydrothermal alteration and mineralization processes that modified the original ferromagnetic mineralogy at differing intensities.
iv. *In-situ* magnetic properties of the HMSG and LMSG do not differ with respect to those observed in formations and units present within the region. Rocks classified within the HRMG have *in-situ* magnetic properties that clearly differ from the country rocks, having a strong NRM over $\chi$.
v. The total variability between HMRG, HMSG, and LMSG occurs within a small cluster of data. This high variability is also seen in other porphyry copper deposits in Chile (*e.g.*, Chuquicamata and El Teniente).
vi. Phyllic, chloritic, and potassic alterations appear to be related to low, intermediate, and high *in-situ* NRM, respectively. High variance may be interpreted as the result of small-scale local hydrothermal processes; hence, the magnetic contrast for a porphyry copper system may not be characterized as a specific magnetic high or low contrast anomaly. These areas are more likely zones of high variance, that is, of a noisy magnetic signal, depending on the scale of the study.

Results from this study indicate that hydrothermal alteration and mineralization processes exert important effects on the magnetic properties of rocks. These mineral transformations also reflect oxidation–reduction processes common to hydrothermal mineral deposits. In the case of porphyry copper deposits, there are significant implications with regard to massive copper-iron sulfide mineralization being related spatially and genetically to the hydrothermal alteration processes and events.

This type of research is fairly new and in-depth studies into porphyry copper and related deposits are recommended, as hydrothermally induced modifications of remanent magnetization may bear relevant implications for mining explorations by means of ground or airborne magnetic surveys.

## Acknowledgements

Our acknowledgements extend to the following people and institutions: Alvio Zuccone and Fernando Gonzales of the Los Pelambres Mine, Mauricio Belmar (microprobe at University of Chile; currently at SGS-Chile), J. Le-Roux (University of Chile) and B. Schneider for English improvement, Natalia Astudillo for helping with the magnetic mineralogy interpretation, IRD for the economic field support, and Sergio Villagrán for his invaluable support during the field component.

## References

Aguirre, L., 1960. Geología de los Andes de Chile Central, Provincia de Aconcagua. Inst. Investig. Geol. Chile 70.
Aguirre, L., Egert, E., 1961. Las formaciones manganesíferas de la región de Quebrada Marquesa, provincia de Coquimbo.
Alva-Valdivia, L., López-Loera, H., 2011. A review of iron oxide transformations, rock magnetism and interpretation of magnetic anomalies: El Morro Mine (Brazil), a case study. Geofís. Int. 50, 341–362.
Alva-Valdivia, L.M., Urrutia-Fucugauchi, J., 1998. Rock magnetic properties and ore microscopy of the iron ore deposit of Las Truchas, Michoacan, Mexico. J. Appl. Geophys. 38, 277–299. http://dx.doi.org/10.1016/S0926-9851(97)00036-0.
Alva-Valdivia, L.M., Rivas, M.L., Goguitchaichvili, A., Urrutia-Fucugauchi, J., Gonzalez, J.A., Morales, J., Gómez, S., Henríquez, F., Nyström, J.O., Naslund, R.H., 2003a. Rock-magnetic

and oxide microscopic studies of the El Laco iron ore deposits, Chilean Andes, and implications for magnetic anomaly modeling. Int. Geol. Rev. 45, 533–547. http://dx.doi.org/10.2747/0020-6814.45.6.533.
Alva-Valdivia, L.M., Rivas, M.L., Gonzalez, A., Goguitchaichvili, A., Urrutia-Fucugauchi, J., Morales, J., Vivallo, W., 2003b. Integrated magnetic studies of the El Romeral iron-ore deposit, Chile: implications for ore genesis and modeling of magnetic anomalies. J. Appl. Geophys. 53, 137–151. http://dx.doi.org/10.1016/S0926-9851(03)00043-0.
Arriagada, C., Roperch, P., Mpodozis, C., 2000. Clockwise block rotations along the eastern border of the Cordillera de Domeyko, Northern Chile (22°45′–23°30′S). Tectonophysics 326, 153–171. http://dx.doi.org/10.1016/S0040-1951(00)00151-7.
Arriagada, C., Roperch, P., Mpodozis, C., Dupont-Nivet, G., Cobbold, P.R., Chauvin, A., Cortés, J., 2003. Paleogene clockwise tectonic rotations in the forearc of central Andes, Antofagasta region, northern Chile. J. Geophys. Res. Solid Earth 108, 2032. http://dx.doi.org/10.1029/2001JB001598.
Astudillo, N., Roperch, P., Townley, B., Arriagada, C., Maksaev, V., 2008. Importance of small-block rotations in damage zones along transcurrent faults. Evidence from the Chuquicamata open pit, Northern Chile. Tectonophysics 450, 1–20. http://dx.doi.org/10.1016/j.tecto.2007.12.008.
Astudillo, N., Roperch, P., Townley, B., Arriagada, C., Chauvin, A., 2010. Magnetic polarity zonation within the El Teniente copper–molybdenum porphyry deposit, central Chile. Mineral. Deposita 45, 23–41. http://dx.doi.org/10.1007/s00126-009-0256-0.
Atkinson, W., Souviron, A., Vehrs, T., Faunes, A., 1996. Geology and mineral zoning of the Los Pelambres porphyry copper deposit, Chile. Econ. Geol., Andean copper deposits new discoveries, mineralization. Styles and Metallogeny 5, 131–154.
Beane, R.E., 1974. Biotite stability in the porphyry copper environment. Econ. Geol. 69, 241–256. http://dx.doi.org/10.2113/gsecongeo.69.2.241.
Beane, R., Titley, S., 1981. In: Skinner, B.J. (Ed.), Porphyry Copper Deposits. Part II, Hydrothermal Alteration and Mineralization. Soc. Econ. Geol. Publ. 1905–1980, pp. 235–269.
Bertens, A., Deckart, K., Gonzalez, A., 2003. Geocronología U-Pb, Re-Os y 40Ar-39Ar del pórfido de Cu-Mo Los Pelambres, Chile central. Presented at the X Congreso Geológico Chileno, Concepción, Chile.
Bertens, A., Clarck, A., Barra, F., Deckart, K., 2006. Evolution of the Los Pelambres-El Pachón porphyry copper-molybdenum district, Chile/Argentina. Presented at the XI Congreso Geológico Chileno, Antofagasta, pp. 179–181.
Brimhall, G.H., 1980. Deep hypogene oxidation of porphyry copper potassium-silicate protore at Butte, Montana; a theoretical evaluation of the copper remobilization hypothesis. Econ. Geol. 75, 384–409. http://dx.doi.org/10.2113/gsecongeo.75.3.384.
Camus, F., 2003. Geología de los sistemas porfíricos de Chile, Servicio Nacional de Geología y Minería. ed. Chile.
Cecioni, G., Westermann, G., 1968. The Triassic/Jurassic marine transition of coastal central Chile. Pac. Geol. 1, 41–75.
Corbett, G., Leach, T., 1998. Southwest pacific rim gold-copper systems: structure, alteration, and mineralization, Society of Economic Geologists. ed, Special Publication.
Faundez, M., 2002. Efectos de los procesos de alteración hidrotermal sobre las propiedades magnéticas de las rocas del yacimiento El Teniente. Universidad de Chile, Santiago, Chile (71 pp.).
Gustafson, L.B., Hunt, J.P., 1975. The porphyry copper deposit at El Salvador, Chile. Econ. Geol. 70, 857–912. http://dx.doi.org/10.2113/gsecongeo.70.5.857.
Hezarkhani, A., Williams-Jones, A.E., Gammons, C.H., 1999. Factors controlling copper solubility and chalcopyrite deposition in the Sungun porphyry copper deposit, Iran. Miner. Deposita 34, 770–783. http://dx.doi.org/10.1007/s001260050237.
Jordan, T.E., Isacks, B.L., Allmendinger, R.W., Brewer, J.A., Ramos, V.A., Ando, C.J., 1983. Andean tectonics related to geometry of subducted Nazca plate. Geol. Soc. Am. Bull. 94, 341–361. http://dx.doi.org/10.1130/0016-7606(1983)94<341:ATRTGO>2.0.CO;2.
Kay, S.M., Ramos, V.A., Marquez, M., 1993. Evidence in Cerro Pampa volcanic rocks for slab-melting prior to ridge-trench collision in southern South America. J. Geol. 101, 703–714.
Kirschvink, J.L., 1980. The least-squares line and plane and the analysis of palaeomagnetic data. Geophys. J. Int. 62, 699–718. http://dx.doi.org/10.1111/j.1365-246X.1980.tb02601.x.
Klemm, L.M., Pettke, T., Heinrich, C.A., Campos, E., 2007. Hydrothermal evolution of the El Teniente deposit, Chile: porphyry Cu-Mo ore deposition from low-salinity magmatic fluids. Econ. Geol. 102, 1021–1045. http://dx.doi.org/10.2113/gsecongeo.102.6.1021.
Krása, D., Herrero-Bervera, E., 2005. Alteration induced changes of magnetic fabric as exemplified by dykes of the Koolau volcanic range. Earth Planet. Sci. Lett. 240, 445–453.
Landtwing, M.R., Pettke, T., Halter, W.E., Heinrich, C.A., Redmond, P.B., Einaudi, M.T., Kunze, K., 2005. Copper deposition during quartz dissolution by cooling magmatic–hydrothermal fluids: the Bingham porphyry. Earth Planet. Sci. Lett. 235, 229–243. http://dx.doi.org/10.1016/j.epsl.2005.02.046.
Lepage, L.D., 2003. ILMAT: an excel worksheet for ilmenite–magnetite geothermometry and geobarometry. Comput. Geosci. 29, 673–678. http://dx.doi.org/10.1016/S0098-3004(03)00042-6.
Lindsley, D.H., 1991. Experimental studies of oxide minerals. Rev. Mineral. Geochem. 25, 69–106.
Lowell, J.D., Guilbert, J.M., 1970. Lateral and vertical alteration-mineralization zoning in porphyry ore deposits. Econ. Geol. 65, 373–408. http://dx.doi.org/10.2113/gsecongeo.65.4.373.
McEnroe, S.A., Robinson, P., Panish, P.T., 2001. Aeromagnetic anomalies, magnetic petrology, and rock magnetism of hemo-ilmenite- and magnetite-rich cumulate rocks from the Sokndal region, South Rogaland, Norway. Am. Mineral. 86, 1447–1468.
McFadden, P.L., McElhinny, M.W., 1988. The combined analysis of remagnetization circles and direct observations in palaeomagnetism. Earth Planet. Sci. Lett. 87, 161–172. http://dx.doi.org/10.1016/0012-821X(88)90072-6.
Meyer, C., Hemley, J., 1997. Wall Rock Alteration, in: Geochemistry of Hydrothermal Ore Deposits. Rinehart and Winstone, New York, pp. 166–232.
O'Reilly, W., 1984. Rock and Mineral Magnetism. Blackie & Son.
Ossandón, G., Fréraut, R., Gustafson, L., Lindsay, D., Zentilli, M., 2001. Geology of the Chuquicamata mine: a progress report. Econ. Geol. 96, 249–270.
Oyarzun, R., Márquez, A., Lillo, J., López, I., Rivera, S., 2014. Giant versus small porphyry copper deposits of Cenozoic age in northern Chile: adakitic versus normal calc-alkaline magmatism. Mineral. Deposita 36, 794–798. http://dx.doi.org/10.1007/s001260100205.
Perelló, J., Sillitoe, R., Mpodozis, C., Brockway, H., Posso, H., 2012. Geologic setting and evolution of the porphyry copper-molybdenum and copper-gold deposits at Los Pelambres, Central Chile. Econ. Geol., Geology and Genesis of Major Copper Deposits and Districts of the World: a Tribute to Richard H. Sillitoe 16, 79/104.
Pollard, P.J., 2006. An intrusion-related origin for Cu–Au mineralization in iron oxide–copper–gold (IOCG) provinces. Mineral. Deposita 41, 179–187. http://dx.doi.org/10.1007/s00126-006-0054-x.
Puochou, L., Pichoir, F., 1984. New model quantitative x-ray microanalysis, I. Application to the analysis of homogeneous samples. Rech. Aero 3, 13–38.
Reed, M., 1997. In: Barnes, H.L. (Ed.), Geochemistry of Hydrothermal Ore Deposits. John Wiley & Sons.
Reich, M., Parada, M.A., Palacios, C., Dietrich, A., Schultz, F., Lehmann, B., 2003. Adakite-like signature of Late Miocene intrusions at the Los Pelambres giant porphyry copper deposit in the Andes of central Chile: metallogenic implications. Mineral. Deposita 38, 876–885. http://dx.doi.org/10.1007/s00126-003-0369-9.
Richards, J.P., 2003. Tectono-magmatic precursors for porphyry Cu-(Mo-Au) deposit formation. Econ. Geol. 98, 1515–1533. http://dx.doi.org/10.2113/gsecongeo.98.8.1515.
Richards, J.P., 2011. Magmatic to hydrothermal metal fluxes in convergent and collided margins. Ore Geol. Rev. 40, 1–26. http://dx.doi.org/10.1016/j.oregeorev.2011.05.006.
Rivano, S., Sepúlveda, P., 1991. Hola Illapel, Región de Coquimbo (Servicio Nacional de Geología y Minería), N° 69.
Rivano, S., Sepúlveda, P., Herve, M., Puig, A., 1985. Cronología K-Ar de las rocas intrusivas entre los 31–32°S, Chile. Rev. Geol. Chile 63–74.
Rivano, S., Godoy, E., Vergara, M., Villarroel, R., 1990. Redefinición de la Formación Farellones en la Cordillera de Los Andes de Chile central (32–34°S). Rev. Geol. Chile 17, 205–214.
Riveros, K., Veloso, E., Campos, E., Menzies, A., Véliz, W., 2014. Magnetic properties related to hydrothermal alteration processes at the Escondida porphyry copper deposit, northern Chile. Mineral. Deposita 49, 693–707.
Sillitoe, R.H., 1973. Geology of the Los Pelambres porphyry copper deposit, Chile. Econ. Geol. 68, 1–10. http://dx.doi.org/10.2113/gsecongeo.68.1.1.
Sillitoe, R.H., 1997. Characteristics and controls of the largest porphyry copper-gold and epithermal gold deposits in the circum-Pacific region. Aust. J. Earth Sci. 44, 373–388. http://dx.doi.org/10.1080/08120099708728318.
Sillitoe, R.H., 2010. Porphyry copper systems. Econ. Geol. 105, 3–41. http://dx.doi.org/10.2113/gsecongeo.105.1.3.
Skewes, A., Atkinson, W., 1985. Petrology of the early formed hydrothermal veins within the central potassic alteration zone of Los Pelambres porphyry copper deposit, Chile. Rev. Geol. Chile 39–56.
Somoza, R., Singer, S., Tomlinson, A., 1999. Paleomagnetic study of upper Miocene rocks from northern Chile: implications for the origin of Late Miocene-Recent tectonic rotations in the southern Central Andes. J. Geophys. Res. Solid Earth 104, 22923–22936. http://dx.doi.org/10.1029/1999JB900215.
Tapia, J., 2005. Alteración hidrotermal y sus efectos sobre propiedades magnéticas de las rocas en el yacimiento tipo pórfido cuprífero Los Pelambres, IV Región, Chile. Universidad de Chile, Santiago (98 pp.).
Tassara, A., Roperch, P., Townley, B., Pavez, A., Sepúlveda, P., 2000. Modificación de las propiedades magnéticas de las rocas en ambientes hidrotermales: 3 ejemplos de la Franja Metalogénica de la Costa, norte de Chile. Presented at the IX Congreso Geológico Chileno, Valdivia, pp. 385–389.
Taylor, G.K., 2000. Palaeomagnetism applied to magnetic anomaly interpretation: a new twist to the search for mineralisation in northern Chile. Mineral. Deposita 35, 377–384. http://dx.doi.org/10.1007/s001260050248.
Townley, B., Roperch, P., Oliveros, V., Tassara, A., Arriagada, C., 2007. Hydrothermal alteration and magnetic properties of rocks in the Carolina de Michilla stratabound copper district, northern Chile. Mineral. Deposita 42, 771–789. http://dx.doi.org/10.1007/s00126-007-0134-6.
Ulrich, T., Günther, D., Heinrich, C.A., 2001. The evolution of a porphyry Cu-Au deposit, based on LA-ICP-MS analysis of fluid inclusions: Bajo de la Alumbrera, Argentina. Econ. Geol. 96, 1743–1774. http://dx.doi.org/10.2113/gsecongeo.96.8.1743.
Vehrs, T., Geologic Staff, Anaconda, S.A, 1982. Exploration and Geologic Evaluation of the Los Pelambres Porphyry Copper Deposit, Chile: Denver, Colorado (Unpublished Report). Anaconda Company.
Vergara, M., Levi, B., Nyström, J.O., Cancino, A., 1995. Jurassic and Early Cretaceous island arc volcanism, extension, and subsidence in the Coast Range of central Chile. Geol. Soc. Am. Bull. 107, 1427–1440. http://dx.doi.org/10.1130/0016-7606(1995)107<1427:JAECIA>2.3.CO;2.